

Feedback-induced nonlinearity and superconducting on-chip quantum opticsZhong-Peng Liu,^{1,2,3,*} Hui Wang,^{2,3,4} Jing Zhang,^{1,2,3,5,†} Yu-xi Liu,^{2,3,4} Re-Bing Wu,^{1,2,3} Chun-Wen Li,^{1,2,3} and Franco Nori^{3,6}¹*Department of Automation, Tsinghua University, Beijing 100084, People's Republic of China*²*Center for Quantum Information Science and Technology, TNLIST, Beijing 100084, People's Republic of China*³*Center for Emergent Matter Science, RIKEN, Saitama 351-0198, Japan*⁴*Institute of Microelectronics, Tsinghua University, Beijing 100084, People's Republic of China*⁵*State Key Laboratory of Robotics, Shenyang Institute of Automation Chinese Academy of Sciences, Shenyang 110016, China*⁶*Physics Department, University of Michigan, Ann Arbor, Michigan 48109-1040, USA*

(Received 26 September 2013; published 30 December 2013)

Quantum coherent feedback has been proven to be an efficient way to tune the dynamics of quantum optical systems and, recently, those of solid-state quantum circuits. Here, inspired by the recent progress of quantum feedback experiments, especially those in mesoscopic circuits, we prove that superconducting circuit QED systems, shunted with a coherent feedback loop, can change the dynamics of a superconducting transmission line resonator, i.e., a linear quantum cavity, and lead to strong on-chip nonlinear optical phenomena. We find that bistability can occur under the semiclassical approximation and photon antibunching can be shown in the quantum regime. Our study presents alternate perspectives for engineering nonlinear quantum dynamics on a chip.

DOI: [10.1103/PhysRevA.88.063851](https://doi.org/10.1103/PhysRevA.88.063851)

PACS number(s): 42.50.Pq, 42.65.Pc, 42.50.Ct, 85.25.—j

I. INTRODUCTION

Feedback, which is the core of modern control theory [1], has been applied to the control of quantum dynamical systems [2–5] for over 20 yr, after Belavkin's pioneering work on quantum filtering and control [6]. It has been extensively studied for various problems in quantum systems, such as optical squeezing [7–9], spin squeezing [10], quantum state stabilization [11–18], quantum error correction and noise suppression [19–26], entanglement control [27–29], cooling [30–33], and rapid quantum measurement [34,35].

There are mainly two different quantum feedback control methods: measurement-based feedback [36–39] and coherent feedback [40–44]. In a typical measurement-based feedback-control optical system, a probe field usually transmits through the quantum system to be controlled and then the information is extracted. Afterward, the extracted information is fed into a classical controller which generates the desired control signal. This control signal is then fed back to tune the dynamics of the controlled system. The simplest measurement-based feedback control protocol is the so-called direct Markovian feedback [36], in which the measurement output is directly fed back to steer the dynamics of the controlled system. Both the time delay in the feedback loop and the filtering effects induced by the integral components are omitted, which leads to the so-called Markovian approximation. However, due to the inevitable time delay and filtering effects in the feedback loop, such a simplification may not be valid in various cases. To solve this problem, another measurement-based feedback protocol, called Bayesian feedback, was proposed [38], in which the measurement output signal is fed into a classical state estimator, e.g., a series of integral components, to estimate the state of the controlled quantum system and then fed into a classical controller to obtain a state-based feedback control.

It is worth noting that both direct Markovian feedback and Bayes feedback have been experimentally demonstrated in optical cavity systems [45–53] and solid-state circuits [24].

Although great progress has been achieved for measurement-based feedback, there are still many problems left to be solved. The main open problems of the measurement-based feedback approaches are that (1) the time scale of the general quantum dynamics is too fast to be manipulated in real time by currently available classical controllers and (2) more essentially the backaction brought by the quantum measurement keeps dumping entropy into the system before the feedback attempts to reduce it. One possible way to solve this is to avoid the introduction of the measurement step and use a fully quantum feedback loop to control the quantum system, which leads to a new feedback mechanism called coherent feedback. The simplest way to introduce coherent feedback is to couple directly the controlled quantum system with the quantum controller [41], which is called direct coherent feedback. An alternative approach is the field-mediated coherent feedback [42–44], in which the controlled quantum system and the quantum controller are connected by an intermediate quantum field. The direction of the information flow in the feedback loop is naturally determined by the propagation direction of the quantum field, and thus it is easier to be realized in experiments [54–58].

The existing studies about coherent feedback are mainly focused on linear quantum systems. This is because previous studies on coherent feedback are mainly focused on quantum optical systems [59], where the nonlinear effects are too weak to be observed. However, recent progress shows that nonlinear quantum optical phenomena induced by the strong interaction between photons and solid-state components can be observed [60–62] in solid-state systems, such as quantum dots, superconducting circuits, and silicon-based waveguides [63–65]. In our previous study [66], we found that, different from measurement-based feedback, quantum coherent feedback can induce and amplify the quantum nonlinear effects and then modulate the dynamics of the controlled system. We call this

*liuzppp@163.com

†jing-zhang@mail.tsinghua.edu.cn

quantum feedback nonlinearization. However, in this study, the quantum nonlinear effects are induced by the nonlinear dissipative coupling between the controlled quantum system and the intermediate quantum field. The quantum feedback loop is just linear.

In this paper, we propose a different nonlinear coherent feedback control strategy and apply it to superconducting circuits. The main difference between this strategy and our previous study in Ref. [66] is that here a nonlinear component, i.e., a nonlinear superconducting device [67–76], is embedded in the feedback loop, and the coupling between the controlled systems and the intermediate quantum field is linear. Such a design might be realizable in future experiments (see, e.g., Ref. [57]).

This paper is organized as follows. In Sec. II, we summarize results from the quantum input-output theory and the theory of coherent feedback-control networks, which will be used here afterward. In Sec. III, we present our design of nonlinear coherent feedback systems in superconducting quantum circuits and then analyze the dynamics of the controlled systems in the semiclassical regime (strong-driving regime) to show bistability in Sec. IV and the quantum regime (weak-driving regime) to show quantum nonlinear optical phenomena, such as photon antibunching effects in Sec. V. Conclusions and discussions are given in Sec. VI.

II. PRELIMINARIES

The basic model for a quantum input-output system can be presented by a controlled system driven by an external bath, where the bath consists of different modes which can be described by a continuum of harmonic oscillators. We assume that $\hbar = 1$ in the following discussions. The Hamiltonian for such a system can be expressed as

$$\begin{aligned} H &= H_{\text{sys}} + H_B + H_{\text{int}}, \\ H_B &= \int_{-\infty}^{+\infty} \omega b^\dagger(\omega) b(\omega) d\omega, \\ H_{\text{int}} &= i \int_{-\infty}^{+\infty} [\kappa(\omega) b^\dagger(\omega) a - \text{H.c.}] d\omega, \end{aligned} \quad (1)$$

where a is the annihilation operator of the system and $b^\dagger(\omega)$ and $b(\omega)$ are the creation and annihilation operators of the bath mode with frequency ω satisfying

$$[b(\omega), b^\dagger(\tilde{\omega})] = \delta(\omega - \tilde{\omega}). \quad (2)$$

The commutator $[\cdot, \cdot]$ is defined as $[A, B] = AB - BA$. H_{sys} is the free Hamiltonian of the system, which interacts with the bath modes with coupling operator a and coupling strengths $\kappa(\omega)$. In the interaction picture, Eq. (1) can be rewritten as

$$H_{\text{eff}} = H_{\text{sys}} + i \int_{-\infty}^{+\infty} [\kappa(\omega) b^\dagger(\omega) e^{i\omega t} a - \text{H.c.}] d\omega. \quad (3)$$

Under the Markov approximation, i.e., when the coupling strength is constant for all frequencies $\kappa(\omega) = \sqrt{\gamma}/2\pi$, the Hamiltonian H_{eff} can be expressed as

$$H_{\text{eff}} = H_{\text{sys}} + i[b_{\text{in}}^\dagger L - L^\dagger b_{\text{in}}]. \quad (4)$$

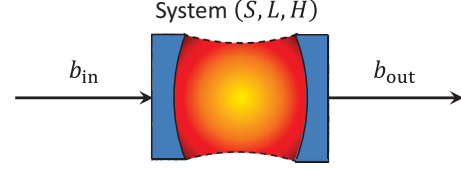


FIG. 1. (Color online) Schematic diagram of the quantum input-output system with the input field b_{in} and the output field b_{out} . Here, S , L , and H are, respectively, the scattering matrices, the Lindblad operator, and the Hamiltonian of the input-output system.

$L = \sqrt{\gamma}a$ is the Lindblad operator induced by the coupling between the system and the quantum field. Also,

$$b_{\text{in}}(t) = \frac{1}{\sqrt{2\pi}} \int_{-\infty}^{+\infty} b(\omega) e^{-i\omega t} d\omega \quad (5)$$

is defined as the input quantum field [77]. Let us consider a general input-output model as in Fig. 1. The input field $b_{\text{in}} = [b_1(t), \dots, b_n(t)]^T$, where the superscript denotes transposition, satisfies the commutation relations $[b_i(t), b_j^\dagger(s)] = \delta_{ij}(t - s)$ and transmits through a beamsplitter described by an $n \times n$ unitary scattering matrix S , such that $S^\dagger S = SS^\dagger = I$. The input field interacts with the controlled system with the Hamiltonian H , which leads to the dissipation channel represented by the Lindblad operator $L = [L_1, \dots, L_n]^T$. The unitary evolution operator $U(t)$ of the total system composed of the controlled system and the input field can be described by the following quantum stochastic differential equation [66,78–80] (see derivations in Appendix A):

$$\begin{aligned} \frac{dU(t)}{dt} &= b_{\text{in}}^\dagger(t)(S - I)U(t)b_{\text{in}}(t) + b_{\text{in}}^\dagger(t)LU(t) \\ &\quad - L^\dagger S U(t)b_{\text{in}}(t) - \left[\frac{1}{2}L^\dagger L - iH \right] U(t), \end{aligned} \quad (6)$$

with initial condition $U(0) = I$, where I is the identity operator. The output field is defined by

$$b_{\text{out}}(t) = U^\dagger(t)S U(t)b_{\text{in}}(t) + U^\dagger(t)LU(t). \quad (7)$$

It can be seen that the above quantum input-output system can be fully determined by a set of operators (S, L, H) . For a quantum Markovian cascaded system as shown in Fig. 2(a), in which the output field of the first component (S_1, L_1, H_1) acts as the input field of the second system (S_2, L_2, H_2) , the dynamics of the total system can be described by

$$(S', L', H'), \quad (8)$$

with

$$\begin{aligned} S' &\equiv S_2 S_1, \quad L' \equiv L_2 + S_2 L_1, \\ H' &\equiv H_1 + H_2 + \frac{i}{2}(L_1^\dagger S_2^\dagger L_2 - L_2^\dagger S_2 L_1). \end{aligned}$$

In particular, we feed the output of the system (S, L, H) back and take it as the input of the same system to construct a direct coherent-feedback network, as in Fig. 2(b). From Eq. (8), such a feedback network can be described by [66]

$$(S, L, H) \quad (9)$$

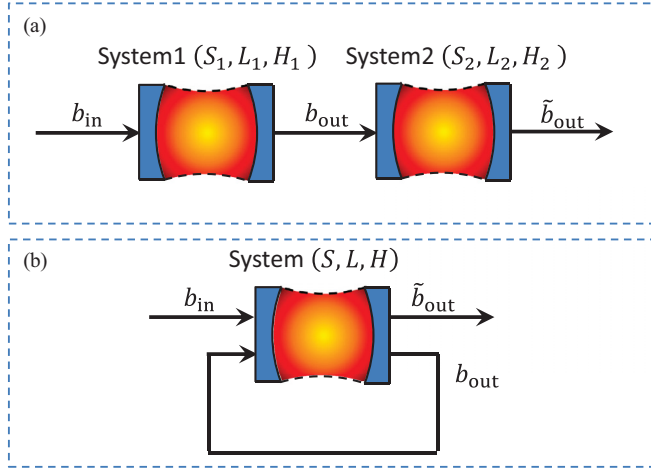


FIG. 2. (Color online) Schematic diagram of the cascade system with two cascaded-connected components in (a) and the feedback-control systems in (b), which can be seen as the controlled system cascaded-connected with itself.

with

$$\begin{aligned}\tilde{S} &\equiv S^2, & \tilde{L} &\equiv L + SL, \\ \tilde{H} &\equiv H + \frac{i}{2}L^\dagger(S^\dagger - S)L.\end{aligned}$$

III. NONLINEAR COHERENT FEEDBACK IN SUPERCONDUCTING CIRCUITS

In Fig. 3 we present our proposed nonlinear coherent feedback system using superconducting circuits. The controlled system is a one-dimensional transmission line resonator (TLR) with distributed inductor L_s and capacitance C_s , which has two input channels and two output channels. The TLR is driven by the input field b_{in} through the dissipation channel represented by the Lindblad operator $L = \sqrt{\gamma}a$. Also a is the annihilation operator of the quantum field in the TLR, and γ is the corresponding dissipation rate. The output field of the TLR is then fed into a controller composed of another TLR coupled to a dc superconducting quantum interference device (SQUID) based superconducting charge qubit, which is driven by either a current or voltage source [81,82]. The quantum controller interacts with the intermediate field via the dissipation channel with Lindblad operator L_c . Afterward, the output of the quantum controller is fed back to act as the input field \tilde{b}_{in} of the controlled system via the dissipation channel L_f to close the coherent feedback loop.

If we assume the inductance of the SQUID to be small, we can neglect the magnetic energy of the circulating currents. Under the two-level approximation, the Hamiltonian of the controller can be expressed as [83]

$$\begin{aligned}H_{qT} &= \frac{1}{2}\omega_0\sigma_z + \omega_c c^\dagger c + g(c\sigma_+ + c^\dagger\sigma_-) \\ &+ \Omega(\sigma_+ e^{-i\omega_1 t} + \sigma_- e^{i\omega_1 t}) + \varepsilon(c^\dagger e^{-i\omega_2 t} + c e^{i\omega_2 t}),\end{aligned}\quad (10)$$

where c is the annihilation operator of the quantized electromagnetic field in the TLR coupled to the dc SQUID based superconducting charge qubit; Ω is the Rabi frequency describing the interaction between the qubit and the classical

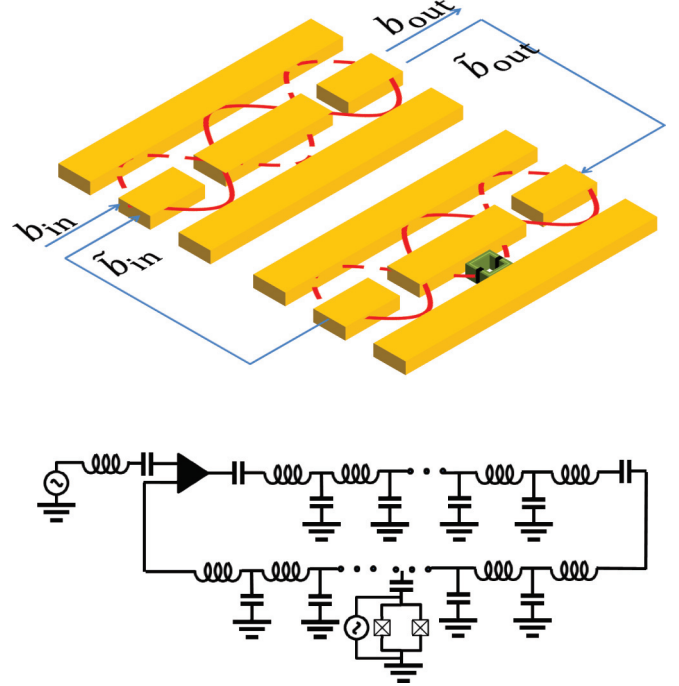


FIG. 3. (Color online) Schematic diagram of the coherent feedback network using superconducting quantum circuits. The controlled system is a TLR which can be considered as a linear cavity. The controller in the feedback loop is another TLR coupled with a dc-SQUID-based superconducting charge qubit which acts as a nonlinear component.

field; g is the coupling strength between the qubit and the quantized electromagnetic field; ω_1 is the frequency of the driving field interacting with the qubit; ω_2 is the frequency of the driving field interacting with the quantized electromagnetic field; and ε is the strength of the driving field applied to the cavity mode. If the Rabi frequency Ω is large enough, such that $\Omega \gg g^2/\Delta_{qT}$, and in the large-detuning regime,

$$\Delta_{qT} = \omega_c - \omega_0 \gg g,$$

we can write an effective Hamiltonian which can be reexpressed as [83] (see derivations in Appendix B)

$$H_{\text{eff}} = \omega_c c^\dagger c + \Omega\sigma_z + \frac{g^4}{2\Omega\Delta_{qT}^2}(c^\dagger c)^2\sigma_z.\quad (11)$$

If the qubit is adiabatically placed in its ground state $|-\rangle$, the effective Hamiltonian in Eq. (11) can be expressed as

$$H'_{qT} = \omega_c c^\dagger c - \chi(c^\dagger c)^2 + \varepsilon(c^\dagger e^{-i\omega_2 t} + c e^{i\omega_2 t}),\quad (12)$$

where $\chi = g^4/(2\Omega\Delta_{qT}^2)$. In the (S, L, H) notation, the quantized electromagnetic field can be represented by

$$(1, \sqrt{\kappa}c, H'_{qT}),\quad (13)$$

where κ is the decay rate of the quantized electromagnetic field. The controlled linear cavity (TLR) can be described as $(1, \sqrt{\gamma}a, \omega_s a^\dagger a)$, where γ and a are the decay rate and the annihilation operator of the cavity, respectively.

The total coherent feedback system can be considered as a cascade system of the subsystem $(1, \sqrt{\gamma}a, \omega_s a^\dagger a)$, the quantum

controller $(1, \sqrt{\kappa}c, H'_{qT})$, and the subsystem $(1, \sqrt{\gamma_f}a, \omega_s a^\dagger a)$, which can be written as

$$(S'', L'', H''), \quad (14)$$

with

$$S'' = 1, \quad L'' = \sqrt{\kappa}c + (\sqrt{\gamma} + \sqrt{\gamma_f})a, \\ H'' = \omega_s a^\dagger a + H'_{qT} + \frac{i}{2}(\sqrt{\kappa\gamma} - \sqrt{\kappa\gamma_f})(a^\dagger c - c^\dagger a).$$

In the rotating reference frame with unitary transformation $V(t) = \exp[i(\omega_2 c^\dagger c + \omega_2 a^\dagger a)t]$, the total Hamiltonian can be represented as

$$H_{\text{tot}} = \Delta_s a^\dagger a + \Delta c^\dagger c - \chi(c^\dagger)^2 c^2 - \varepsilon(c^\dagger + c) \\ + \frac{i}{2}(\sqrt{\kappa\gamma} - \sqrt{\kappa\gamma_f})(a^\dagger c - c^\dagger a), \quad (15)$$

where

$$\Delta_s = \omega_s - \omega_2, \quad \Delta = \omega_c - \omega_2$$

are the detuning frequencies.

With the decrease of the strength of the external driving field, different optical phenomena can be observed. In the strong-driving semiclassical regime semiclassical nonlinear bistability effects can be found, while in the weak-driving quantum regime quantum nonlinear phenomena such as antibunching can be observed.

IV. NONLINEAR ON-CHIP OPTICS BY COHERENT FEEDBACK: SEMICLASSICAL REGIME

We first consider the case in which the external field imposed on the controller is strong, where we can observe semiclassical nonlinear phenomena such as optical bistability. Optical bistability is a typical nonlinear phenomenon which has been observed in various systems [84–89]. It has also been demonstrated that quantum feedback can modulate such kinds of nonlinear effects. For example, the recent experiment [57] showed that two coupled superconducting tunable Kerr cavities (TKCs) connected in a feedback configuration can demonstrate semiclassical on-chip nonlinear optical phenomena. The reflected phase from the TKC is a nonlinear function of the driving amplitude and thus the TKC acts as a typical nonlinear component, which means that both the controlled system and the controller are nonlinear systems. In contrast to this design, in our system, as shown in Fig. 3, the controlled system is a linear system and the controller is nonlinear. We now want to show how the nonlinear controller modulates the controlled linear dynamics, making the controlled system nonlinear.

Based on the Hamiltonian in Eq. (15), the Heisenberg-Langevin equations of the total system can be described by

$$\dot{a} = -i\Delta_s a - \frac{1}{2}(\sqrt{\gamma} + \sqrt{\gamma_f})^2 a - \sqrt{\kappa\gamma_f}c \\ - (\sqrt{\gamma} + \sqrt{\gamma_f})b_{\text{in}}, \quad (16)$$

$$\dot{c} = -i\Delta c + i\chi(2c^\dagger c c) - \frac{\kappa}{2}c - \sqrt{\kappa\gamma}a \\ + i\varepsilon - \sqrt{\kappa}b_{\text{in}}, \quad (17)$$

where b_{in} is the vacuum field with zero mean value $\langle b_{\text{in}}(t) \rangle = 0$ and delta correlation $\langle b_{\text{in}}(t)b_{\text{in}}^\dagger(t') \rangle = \delta(t-t')$, where $\langle \cdot \rangle$ represents the average over the equilibrium state of the environment. The input-output relation of the total system can be written as

$$b_{\text{out}} = (\sqrt{\gamma_f} + \sqrt{\gamma})a + \sqrt{\kappa}c + b_{\text{in}}. \quad (18)$$

Using the mean-field approximation, the time evolutions of the mean values of the operators a and c can be given by [90]

$$\frac{d\langle a \rangle}{dt} = -i\Delta_s \langle a \rangle - \frac{1}{2}(\sqrt{\gamma} + \sqrt{\gamma_f})^2 \langle a \rangle - \sqrt{\kappa\gamma_f} \langle c \rangle, \\ \frac{d\langle c \rangle}{dt} = -i\Delta \langle c \rangle + i\chi(2\langle c^\dagger \rangle \langle c \rangle^2) - \frac{\kappa}{2} \langle c \rangle \\ - \sqrt{\kappa\gamma} \langle a \rangle + i\varepsilon. \quad (19)$$

By assuming that the steady values of $\langle a \rangle$ and $\langle c \rangle$ are A_0 and C_0 , we can obtain A_0 and C_0 by the following equations:

$$4\chi^2 |C_0|^6 - 4p_2 \chi |C_0|^4 + (p_1^2 + p_2^2) |C_0|^2 = |\varepsilon|^2, \quad (20)$$

$$|A_0|^2 = \frac{4\kappa\gamma_f}{4\Delta_s^2 + (\sqrt{\gamma} + \sqrt{\gamma_f})^4} |C_0|^2,$$

with

$$p_1 = \frac{\kappa}{2} - \frac{2\kappa\sqrt{\gamma\gamma_f}(4\sqrt{\gamma} + \sqrt{\gamma_f})^2}{4\Delta_s^2 + (\sqrt{\gamma} + \sqrt{\gamma_f})^4},$$

$$p_2 = \Delta + \frac{4\kappa\sqrt{\gamma\gamma_f}\Delta_s}{4\Delta_s^2 + (\sqrt{\gamma} + \sqrt{\gamma_f})^4}.$$

When $p_2 > \sqrt{3}p_1$, Eq. (20) has two stable solutions corresponding to a local maximum and a local minimum, respectively, which means that the system is in a bistable regime. Indeed, the maximum of $|C_0|^2$ can be found by $\partial|C_0|^2/\partial\Delta = 0$, which leads to

$$-2\chi |C_0|^2 + p_2 = 0. \quad (21)$$

Substituting Eq. (21) into Eq. (20), we can obtain

$$|\varepsilon|^2 = p_1^2 |C_0|^2, \quad (22)$$

by which we can find the strength of the driving field that maximizes the intracavity intensity for fixed Δ . Additionally, we also know that the bifurcation line with the current drive and detuning parameter which provides the boundary between the single-solution and bistable-solution regions is located where the susceptibility $\partial C/\partial\Delta$ diverges, where $C = |C_0|^2$. The bistability occurs when $\partial\Delta/\partial C = \partial^2\Delta/\partial C^2 = 0$ holds. This condition leads to $12\chi^2 C^2 - 8p_2\chi C + p_1^2 + p_2^2 = 0$ and $3\chi^2 C - p_2\chi = 0$. Thus, it is easy to find that the critical point of bistability $p_2^2 = 3p_1^2$ (from which we find that $|p_2| > \sqrt{3}|p_1|$ and $C > \sqrt{3}|p_1|/\chi$) should be satisfied to remain in the stable region. Substituting these into Eq. (22), we relate p_1 and the driving field intensity ε in the stable region with a maximum intracavity intensity as

$$|\varepsilon|^2 > \frac{\sqrt{3}p_1^3}{\chi}. \quad (23)$$

From Fig. 4, we find there is a two-steady-state relation between the steady-state solution for the controlled system

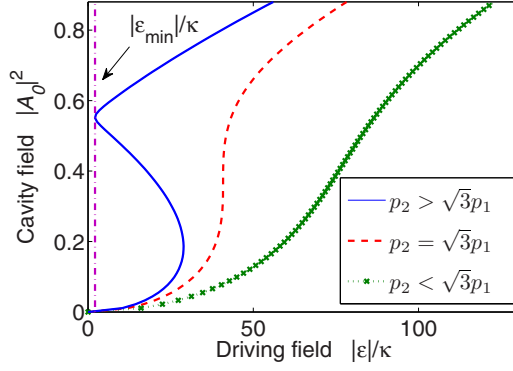


FIG. 4. (Color online) Magnitude of the steady field $|A_0|^2$ in the controlled cavity vs the intensity of the driving field $|\varepsilon|$, with system parameters $\Delta_s/2\pi = 100$ MHz, $\Delta/2\pi = 4.9$ MHz, $\chi/2\pi = 10$ MHz, $\gamma/2\pi = 6$ MHz, $\gamma_f/2\pi = 8$ MHz, and $\kappa/2\pi = 3$ MHz. In the parameter regime $p_2 > \sqrt{3}p_1$, we observe a hysteresis curve, indicating bistability. In the parameter regime $p_2 \leq \sqrt{3}p_1$, bistability disappears.

and driving intensity, where $|\varepsilon|^2 > \sqrt{3}p_1^3/\chi$, and the two steady-state solutions can be lost when $|\varepsilon|^2 \leq \sqrt{3}p_1^3/\chi$.

V. NONLINEAR ON-CHIP OPTICS BY COHERENT FEEDBACK: QUANTUM REGIME

We now consider the case in which the external field imposed on the controller is weak. In this case, the controlled system is in the full quantum regime. Under the Markovian approximation, the evolution of the total system can be described by the following master equation [91]:

$$\frac{d\rho}{dt} = -i[H_{\text{tot}}, \rho] + \frac{1}{2}(2L_{\text{tot}}\rho L_{\text{tot}}^\dagger - L_{\text{tot}}^\dagger L_{\text{tot}}\rho - \rho L_{\text{tot}}^\dagger L_{\text{tot}}), \quad (24)$$

where the Lindblad operator L_{tot} can be represented as

$$L_{\text{tot}} = (\sqrt{\gamma} + \sqrt{\gamma_f})a + \sqrt{\kappa}c.$$

From Eq. (24), we obtain the steady state ρ_{ss} by letting $d\rho/dt = 0$, and thus we can calculate the following normalized second-order correlation function of the controlled system:

$$g^{(2)}(0) = \frac{\langle (a^\dagger)^2 a^2 \rangle}{\langle a^\dagger a \rangle^2} \equiv \frac{\text{Tr}(\rho_{\text{ss}}(a^\dagger)^2 a^2)}{[\text{Tr}(\rho_{\text{ss}} a^\dagger a)]^2}, \quad (25)$$

which provides the information of the photon number statistics of the single-mode cavity field in the TLR. Let us define a new parameter $K = \Delta/\chi + 1$, which can be tuned by adjusting the detuning Δ , where values of $K = 1$ and 2 mean that the system is in the single-photon and two-photon blockade regimes [92]. We compare the numerical and analytical solutions of $g^{(2)}(0)$ in Fig. 5. The analytical solution of $g^{(2)}(0)$ is obtained in the following way. From Eq. (25), we have [93]

$$g^{(2)}(0) = \frac{\sum_n n(n-1)P_n}{(\sum_n nP_n)^2}, \quad (26)$$

where P_n represents the probability with n photons. In the weak-driving limit, i.e., $\varepsilon \rightarrow 0$, it can be shown that $P_n \gg$

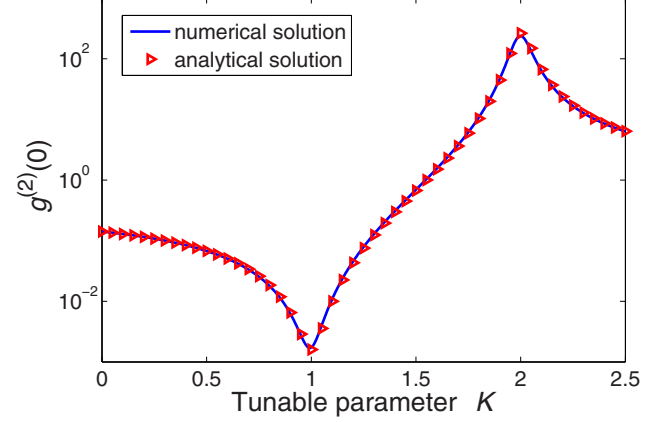


FIG. 5. (Color online) The numerical and analytical solutions for the second-order correlation function $g^{(2)}(0)$ in Eq. (25) vs the tunable parameter K . The system parameters for this simulation are $\chi = 10$ MHz, $\Delta_s = 50$ MHz, $\gamma/2\pi = 2$ MHz, $\gamma_f/2\pi = 2.5$ MHz, $\kappa = 1$ MHz, and $\varepsilon = 0.1\kappa$.

P_{n+1} for $n \geq 2$. Thus, we can omit the probability for three or more photons. In this case, the steady state of the system can be expressed as

$$|\psi\rangle = \sum_{n_p=0}^2 \sum_{n_c=0}^2 C_{n_p, n_c} |n_p, n_c\rangle, \quad (27)$$

where $|n_p\rangle$ and $|n_c\rangle$ are the states of the controlled system and the controller, respectively. In order to find the coefficients C_{n_p, n_c} for the steady state, we introduce the complex Hamiltonian by letting

$$\begin{aligned} \Delta_s &\rightarrow \Delta_s - i(\sqrt{\gamma} + \sqrt{\gamma_f})^2/2, \\ \Delta &\rightarrow \Delta - i\kappa/2 \end{aligned}$$

represent the dissipation effects. Then, the steady state can be found via $d|\psi(t)\rangle/dt = 0$. The probability of the n_p th occupation number can be expressed as

$$P_{n_p} = \sum_{n_c} |C_{n_p, n_c}|^2.$$

Thus, in the weak-driving limit, $g^{(2)}(0)$ can be described by (see derivations in Appendix C)

$$g^{(2)}(0) = \frac{|\Delta_s + (K-2)\chi - \frac{i}{2}\gamma_a|^2 |(K-1)\chi - \frac{i}{2}\kappa|^2}{\left[|(K-2)\chi - \frac{i}{2}\kappa| \left|\Delta_s + (K-1)\chi - \frac{i}{2}\gamma_a\right|\right]^2}, \quad (28)$$

with

$$\gamma_a = (\sqrt{\gamma} + \sqrt{\gamma_f})^2 + \kappa.$$

In Fig. 5, the analytical result for $g^{(2)}(0)$ fits well with the numerical solution obtained by the few photon truncation in the weak-driving regime. It can be shown that

$$g^{(2)}(0) = \frac{4\kappa^2(\Delta_s - \chi)^2 + \kappa^2\gamma_a^2}{4\kappa^2\Delta_s^2 + 16\chi^2\Delta_s^2 + (4\chi^2 + \kappa^2)\gamma_a^2}, \quad (29)$$

when $K = 1$. When the dissipation coefficients κ , γ , and γ_f are far less than the Kerr nonlinear coefficient χ and the detuning

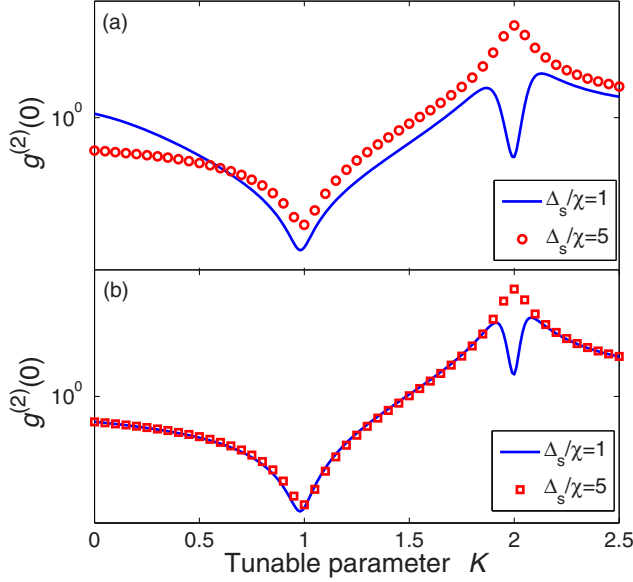


FIG. 6. (Color online) (a) $g^{(2)}(0)$ for the controlled TLR and (b) $g^{(2)}(0)$ for the controller vs the parameter $K = \Delta_s/\chi + 1$. The red dotted curve and the blue curve correspond to different detuning frequencies $\Delta_s = 50$ and 10 MHz. The other system parameters are $\chi = 10$ MHz, $\gamma/2\pi = 2$ MHz, $\gamma_f/2\pi = 2.5$ MHz, $\kappa = 1$ MHz, and $\varepsilon = 0.1\kappa$.

frequency Δ_s , we have $g^{(2)}(0) < 1$, which leads to the single-photon blockade. We plot the curve of $g^{(2)}(0)$ for the controlled single-mode cavity in the TLR in Fig. 6(a). We find that there is a minimum point of $g^{(2)}(0)$ at $K = 1$ for each curve, which means that photon antibunching occurs. This typical nonlinear quantum phenomenon observed in the linear-controlled single-mode cavity in the TLR is induced by the Kerr nonlinearity in the controller by coherent feedback.

However, the curves for different detuning frequencies Δ_s are different at $K = 2$. For $\Delta_s/\chi = 1$, we can observe that $g^{(2)}(0) < 1$, which means that photon blockade occurs. In this case, it can be shown from $K = 2$ and $\Delta_s/\chi = 1$ that $\omega_s = \omega_c$, which means that the controller and the controlled TLR resonate with each other. When the resonance occurs, if one photon enters the controlled TLR, this photon will be transmitted to the controller from the feedback loop and then transmitted back. It will block the next photon to enter the controlled TLR. In Fig. 6(b), we can find for the curve with $\Delta_s/\chi = 5$ that $g^{(2)}(0) > 1$ at $K = 2$, which means two photons resonating. This corresponds to a transparency effect.

In Fig. 7, we show how $g^{(2)}(0)$ depends on the parameters K and Δ_s . The photon antibunching occurs at $K = 1$ with any Δ_s . However, at $K = 2$ it can only be observed when $\Delta_s/\chi = 1$, which means that the controlled TLR and the controller are resonant with each other.

In Fig. 8, we also study how $g^{(2)}(0)$ depends on the strength of the driving field. In Fig. 8(a), we find that $g^{(2)}(0) \rightarrow 1$ when increasing the strength of the driving field. We can also observe that $g^{(2)}(0)$ is minimized when the resonance occurs, i.e., $\Delta_s/\chi = 1$. Similar to Fig. 8(a), in Fig. 8(b) we find that all the curves converge to 1 when increasing the strength of the

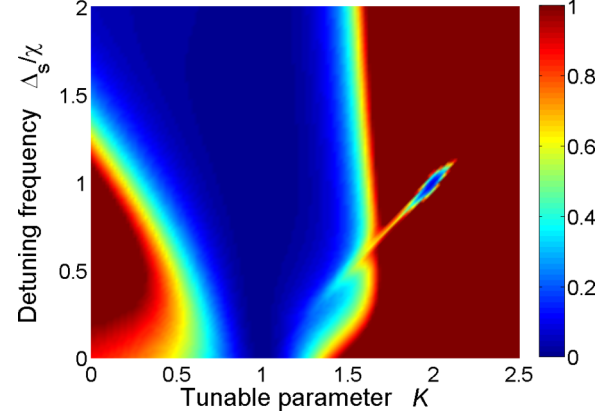


FIG. 7. (Color online) Second-order correlation function vs K and Δ_s , with $\chi = 10$ MHz, $\gamma/2\pi = 2$ MHz, $\gamma_f/2\pi = 2.5$ MHz, $\kappa = 1$ MHz, and $\varepsilon = 0.1\kappa$. Note that $g^{(2)}(0) < 1$ occurs when $\Delta_s - (K - 1)\kappa = 0$, namely, $\omega = \omega_s$ and $K = 1$ with any Δ_s .

driving field. However, we can obtain a concave curve when the resonance occurs, i.e., $\Delta_s/\chi = 1$.

The generated nonlinear effects in the controlled single-mode field in the TLR can be enhanced by increasing the nonlinear strength of the controller, and the nonlinear strength χ of the controller can be tuned by adjusting the detuning frequency Δ_{qT} . Thus, we can enhance the generated nonlinear effects in the controlled TLR by tuning Δ_{qT} . Indeed, from Fig. 9, we can find that the antibunching effects in the controlled TLR are enhanced by decreasing the detuning Δ_{qT} .

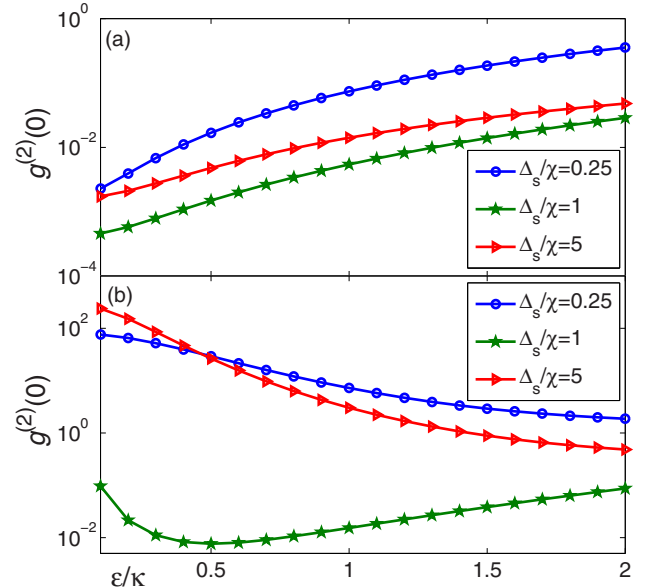


FIG. 8. (Color online) Second-order correlation function vs the normalized driving strength ε/κ , for different values of the detuning frequency Δ_s . Here the system parameters are $\chi = 10$ MHz, $\gamma/2\pi = 2$ MHz, $\gamma_f/2\pi = 2.5$ MHz, and $\kappa = 1$ MHz. (a) $K = 1$. (b) $K = 2$.

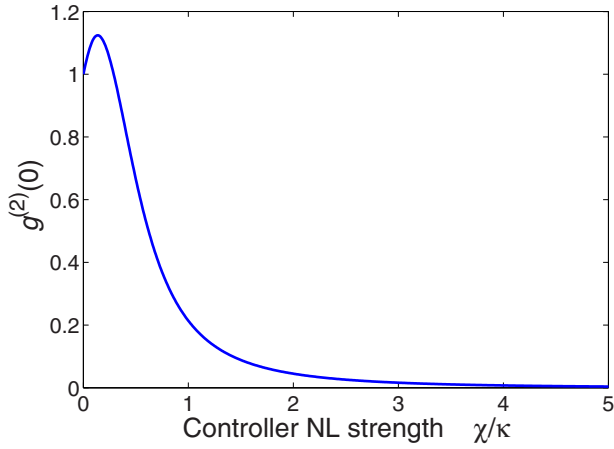


FIG. 9. (Color online) Second-order correlation function vs the nonlinear strength χ of the controller, where the parameters of the system are $K = 1$, $\gamma/2\pi = 2$ MHz, $\gamma_f/2\pi = 2.5$ MHz, $\kappa = 1$ MHz, and $\varepsilon = 0.1\kappa$.

VI. CONCLUSIONS

In summary, we presented a nonlinear coherent feedback-control system in superconducting circuits in which a controlled linear transmission line resonator is modulated by another transmission line resonator coupled to a dc SQUID based superconducting charge qubit in the feedback loop. Such a design changes the linear dynamics of the controlled resonator and makes it nonlinear. This nonlinear coherent feedback-control system is used to produce strong nonlinear on-chip optical phenomena. In the semiclassical regime, we observe in simulations bistable optical-type phenomena observed in previous optical experiments and give the condition to observe this bistability.

In the quantum regime, we predict a photon antibunching induced by nonlinear coherent feedback, which is believed to be a typical quantum optics phenomenon that violates the Cauchy-Schwartz inequality for classical light. Our study shows that dynamics of a linear system can be switched to that of a nonlinear one by using nonlinear coherent feedback in a controllable way. We hope that our prediction of nonlinear coherent feedback in the quantum regime can be verified experimentally in the near future.

ACKNOWLEDGMENTS

ZPL would like to thank Dr. X.W. Xu for helpful discussions. JZ and RBW are supported by the National Natural Science Foundation of China (NSFC) under Grants No. 61174084, No. 61134008, and No. 60904034 and a project supported by the State Key Laboratory of Robotics, Shenyang Institute of Automation Chinese Academy of Sciences, China. YXL is supported by the NSFC under Grants No. 61025022 and No. 60836001. FN is partially supported by the ARO, RIKEN iTHES Project, Multidisciplinary University Research Initiative Center for Dynamic Magneto-Optics, JSPS-RFBR Contract No. 12-02-92100, Grant-in-Aid for Scientific Research (S), Ministry of Education, Culture, Sports, Science and Technology Kakenhi on Quantum Cybernetics, and the

Japan Society for the Promotion of Science via its FIRST program.

APPENDIX A: QUANTUM STOCHASTIC DIFFERENTIAL EQUATION

The mathematical theory of the quantum stochastic differential equation we consider here can be found in Ref. [80], and its applications to quantum optical systems are described in Ref. [78]. The quantum stochastic terms are induced by the zero-point fluctuation of the input field, which leads to the theory of quantum noncommutable probability [80]. This is in contrast to the classical commutable probability theory. In Ref. [78], a so-called quantum Wiener process is defined by

$$B_{\text{in}}(t) = \int_{t_0}^t b_{\text{in}}(s) ds, \quad (\text{A1})$$

with b_{in} as the input field. This leads to a set of quantum Itô rules for the increment of $B_{\text{in}}(t)$:

$$\begin{aligned} dB_{\text{in}}(t)dB_{\text{in}}^\dagger(t) &= dt, \\ dB_{\text{in}}^\dagger(t)dB_{\text{in}}(t) &= dB_{\text{in}}(t)dB_{\text{in}}(t) = dB_{\text{in}}^\dagger(t)dB_{\text{in}}^\dagger(t) = 0. \end{aligned} \quad (\text{A2})$$

To derive Eq. (6), we would like to derive its differential form:

$$\begin{aligned} dU(t) &= \{\text{tr}[(S - I)d\Lambda^T] + dB_{\text{in}}^\dagger L - L^\dagger S dB_{\text{in}} \\ &\quad - \frac{1}{2}L^\dagger L dt - iH dt\}U(t), \end{aligned} \quad (\text{A3})$$

where $\Lambda(t) = \int_0^t b_{\text{in}}^\dagger(s)b_{\text{in}}(s)ds$ is the matrix of the gauge processes with matrix element Λ_{ij} as the gauge process for destructing a photon in channel j and creating a photon in channel i , and the transpose Λ^T is defined by $\Lambda^T = \{\Lambda_{ji}\}$. The increments of $\Lambda(t)$ and the quantum Wiener process $B_{\text{in}}(t)$ satisfy the following extended quantum Itô rule:

$$\begin{aligned} dB_{\text{in}}^\dagger(t) d\Lambda(t) &= dB_{\text{in}}^\dagger(t), \\ d\Lambda(t) d\Lambda(t) &= d\Lambda(t), \\ d\Lambda(t) dB_{\text{in}}^\dagger(t) &= dB_{\text{in}}^\dagger(t). \end{aligned} \quad (\text{A4})$$

The quantum input-output component given by Eq. (A3) can be decomposed as a quantum input-output component with identity scattering matrix and a beamsplitter with scattering matrix S . Let us first consider a quantum input-output component with identity scattering matrix. The Hamiltonian for such a system can be expressed as Eq. (1), and, in the interaction picture, the effect Hamiltonian H_{eff} can be expressed as Eq. (4). It can be verified from the Itô rule Eq. (A2) that the evolution operator U_1 of such a quantum input-output component can be expressed as

$$dU_1 = [LdB_{\text{in}} - dB_{\text{in}}^\dagger L - (\frac{1}{2}L^\dagger L + iH_{\text{sys}})dt]U_1. \quad (\text{A5})$$

For a beamsplitter with scattering matrix S , let us assume that its unitary evolution operator U_2 satisfies the following equation:

$$dU_2 = (A dt + B dB_{\text{in}} + C dB_{\text{in}}^\dagger + D d\Lambda)U_2 = (dG)U_2, \quad (\text{A6})$$

where A, B, C, D are parameters that need to be determined. The quantum field transmitting through a beamsplitter evolves according to

$$B_{\text{out}} = U_2^\dagger B_{\text{in}} U_2, \quad (\text{A7})$$

and the relationship between dB_{out} and dB_{in} is

$$dB_{\text{out}} = S dB_{\text{in}}. \quad (\text{A8})$$

From Eq. (A7), we have

$$dB_{\text{out}} = (1 + dG^\dagger) dB_{\text{in}} (1 + dG). \quad (\text{A9})$$

By comparing Eqs. (A8) and (A9), we can solve the parameter A, B, C, D in dG and thus obtain

$$dU_2 = (S - I)U_2 d\Lambda. \quad (\text{A10})$$

From Eqs. (A5) and (A10), we can obtain the evolution of the total system $U = U_2 U_1$ by

$$dU = (dU_2)U_1 + U_2(dU_1) + (dU_2)(dU_1), \quad (\text{A11})$$

which is Eq. (A3).

APPENDIX B: QUBIT-INDUCED NONLINEARITY

If the detuning frequency $\Delta_{qT} = \omega_c - \omega_0$ between the qubit and the TLR is much larger than the intensity g between the qubit and the TLR, by making the unitary transformation

$$U_0 = \exp\left[\frac{g}{\Delta_{qT}}(c\sigma_+ - c^\dagger\sigma_-)\right], \quad (\text{B1})$$

the effective Hamiltonian can be described as

$$\begin{aligned} H_{\text{eff}} &= U_0 H U_0^\dagger \\ &\approx \left(\omega_c + \frac{g^2}{\Delta_{qT}}\sigma_z\right) c^\dagger c + \frac{1}{2} \left(\omega_0 + \frac{g^2}{\Delta_{qT}}\right) \sigma_z \\ &\quad + \Omega(\sigma_+ e^{-i\omega_1 t} + \sigma_- e^{i\omega_1 t}). \end{aligned} \quad (\text{B2})$$

In the rotating reference frame with frequency ω_1 of the driving field, we let

$$U_1 = \exp\left[-i\omega_1 \frac{\sigma_z}{2}\right] t, \quad (\text{B3})$$

where $\omega_1 = \omega_0 + \frac{g^2}{\Delta_{qT}}$; the Hamiltonian can then be described by

$$H'_{\text{eff}} = \omega_c c^\dagger c + \Omega\sigma_x + \frac{g^2}{\Delta_{qT}} c^\dagger c \sigma_z. \quad (\text{B4})$$

We set $\sigma_z \rightarrow \sigma_x$, and then

$$H''_{\text{eff}} = \omega_c c^\dagger c + \Omega\sigma_z + \frac{g^2}{\Delta_{qT}} c^\dagger c (\sigma_+ + \sigma_-). \quad (\text{B5})$$

If the Rabi frequency Ω satisfies the condition $\Omega \gg (g^2/\Delta_{qT})$, through the unitary transformation

$$U_2 = \exp\left[\frac{g^2}{2\Omega\Delta_{qT}} c^\dagger c (\sigma_+ - \sigma_-)\right], \quad (\text{B6})$$

the Hamiltonian can be reexpressed by

$$H'''_{\text{eff}} = \omega_c c^\dagger c + \Omega\sigma_z + \frac{g^4}{2\Omega\Delta_{qT}^2} (c^\dagger c)^2 \sigma_z. \quad (\text{B7})$$

APPENDIX C: DERIVATION OF THE SECOND-ORDER CORRELATION FOR THE CONTROLLED SYSTEM

In the limit of a weak-driving field, the state $|\psi\rangle$ can be derived using perturbation theory. In order to show explicitly the second-order correlation, up to second order in $|\varepsilon|$, we set $|\psi\rangle = C_{00}|00\rangle + C_{01}|01\rangle + C_{02}|02\rangle + C_{10}|10\rangle + C_{11}|11\rangle + C_{12}|12\rangle + C_{20}|20\rangle + C_{21}|21\rangle + C_{22}|22\rangle$. The steady solution for the coefficients $C_{n_a n_c}$ can be given by the Schrödinger equation for $|\psi\rangle$, when the limit of neglecting pure dephasing is neglected:

$$i \frac{d|\psi\rangle}{dt} = H_{\text{tot}} |\psi\rangle, \quad (\text{C1})$$

assuming $d|\psi(t)\rangle/dt = 0$, and

$$0 = \Delta_s C_{10} - \varepsilon C_{11} + \frac{i}{2}(\sqrt{\kappa\gamma} - \sqrt{\kappa\gamma_f}) C_{01}, \quad (\text{C2})$$

$$0 = \Delta_s C_{10} - \varepsilon C_{11} + \frac{i}{2}(\sqrt{\kappa\gamma} - \sqrt{\kappa\gamma_f}) C_{01}, \quad (\text{C3})$$

$$\begin{aligned} 0 &= (\Delta_s + \Delta) C_{11} - \varepsilon C_{10} - \sqrt{2}\varepsilon C_{12} \\ &\quad + \frac{i}{\sqrt{2}}(\sqrt{\kappa\gamma} - \sqrt{\kappa\gamma_f}) C_{02} - \frac{i}{\sqrt{2}}(\sqrt{\kappa\gamma} - \sqrt{\kappa\gamma_f}) C_{20}, \end{aligned} \quad (\text{C4})$$

$$0 = (\Delta_s + 2\Delta - 2\chi) C_{12} - \sqrt{2}\varepsilon C_{11} - i(\sqrt{\kappa\gamma} - \sqrt{\kappa\gamma_f}) C_{21}, \quad (\text{C5})$$

$$0 = -\varepsilon C_{00} - \sqrt{2}\varepsilon C_{02} - \frac{i}{2}(\sqrt{\kappa\gamma} - \sqrt{\kappa\gamma_f}) C_{10} + \Delta C_{01}, \quad (\text{C6})$$

$$0 = (2\Delta - 2\chi) C_{02} - \sqrt{2}\varepsilon C_{01} - \frac{i}{\sqrt{2}}(\sqrt{\kappa\gamma} - \sqrt{\kappa\gamma_f}) C_{11}, \quad (\text{C7})$$

$$\begin{aligned} 0 &= (2\Delta_s + \Delta) C_{21} - \varepsilon C_{20} - \sqrt{2}\varepsilon C_{22} \\ &\quad + i(\sqrt{\kappa\gamma} - \sqrt{\kappa\gamma_f}) C_{12}, \end{aligned} \quad (\text{C8})$$

$$0 = 2\Delta_s C_{20} - \varepsilon C_{21} + \frac{i}{\sqrt{2}}(\sqrt{\kappa\gamma} - \sqrt{\kappa\gamma_f}) C_{11}, \quad (\text{C9})$$

$$0 = (2\Delta_s + 2\Delta - 2\chi) C_{22} - \sqrt{2}\varepsilon C_{21}. \quad (\text{C10})$$

Due to the weak limit of the driving field, we can assume $C_{00} \rightarrow 1$, and the equations are now closed (i.e., nine equations

for nine parameters). Thus, it is possible to obtain the analytical solution of the system. However, the solution is cumbersome, but we can neglect the higher order terms in $|\varepsilon|$, obtaining

$$P_1 = |C_{10}|^2 + |C_{11}|^2 + |C_{12}|^2 \approx \frac{|(\sqrt{\kappa\gamma} - \sqrt{\kappa\gamma_f})\varepsilon|^2}{|(\Delta - \chi)\Delta_s|^2}, \quad (\text{C11})$$

$$P_2 = |C_{20}|^2 + |C_{21}|^2 + |C_{22}|^2 \approx \frac{|(\sqrt{\kappa\gamma} - \sqrt{\kappa\gamma_f})\varepsilon|^4 |\Delta_s - 2\chi + \Delta|^2}{2|(\Delta - \chi)(\Delta - 2\chi)(\Delta_s + \Delta - \chi)\Delta_s^2|^2}. \quad (\text{C12})$$

We substitute Eqs. (C11) and (C12) into Eq. (26), and then we can derive the analytical solution of the $g^{(2)}(0)$ in the form of Eq. (28).

-
- [1] K. J. Åström and R. M. Murray, *Feedback Systems: An Introduction for Scientists and Engineers* (Princeton University Press, Princeton, NJ, 2008).
- [2] H. M. Wiseman and G. J. Milburn, *Quantum Measurement and Control* (Cambridge University Press, Cambridge, England, 2009).
- [3] D. Y. Dong and I. R. Petersen, *IET Control Theory and Applications* **4**, 2651 (2010).
- [4] C. Altafini and F. Ticozzi, *IEEE Trans. Automat. Contr.* **57**, 1898 (2012).
- [5] J. Kerckhoff, R. W. Andrews, H. S. Ku, W. F. Kindel, K. Cicak, R. W. Simmonds, and K. W. Lehnert, *Phys. Rev. X* **3**, 021013 (2013).
- [6] V. P. Belavkin, *J. Multivariate Anal.* **42**, 171 (1992); *Commun. Math. Phys.* **146**, 611 (1992); *Theor. Probab. Appl.* **38**, 573 (1993).
- [7] H. M. Wiseman and G. J. Milburn, *Phys. Rev. A* **49**, 1350 (1994).
- [8] J. E. Gough and S. Wildfeuer, *Phys. Rev. A* **80**, 042107 (2009).
- [9] S. Iida, M. Yukawa, H. Yonezawa, N. Yamamoto, and A. Furusawa, *IEEE Trans. Automat. Contr.* **57**, 2045 (2012).
- [10] L. K. Thomsen, S. Mancini, and H. M. Wiseman, *Phys. Rev. A* **65**, 061801 (2002).
- [11] J. Wang and H. M. Wiseman, *Phys. Rev. A* **64**, 063810 (2001).
- [12] J. K. Stockton, R. van Handel, and H. Mabuchi, *Phys. Rev. A* **70**, 022106 (2004).
- [13] R. van Handel, J. K. Stockton, and H. Mabuchi, *IEEE Trans. Automat. Contr.* **50**, 768 (2005).
- [14] P. Campagne-Ibarcq, E. Flurin, N. Roch, D. Darson, P. Morfin, M. Mirrahimi, M. H. Devoret, F. Mallet, and B. Huard, *Phys. Rev. X* **3**, 021008 (2013).
- [15] G. Kießlich, G. Schaller, C. Emary, and T. Brandes, *Phys. Rev. Lett.* **107**, 050501 (2011).
- [16] G. Kießlich, C. Emary, G. Schaller, and T. Brandes, *New J. Phys.* **14**, 123036 (2012).
- [17] G. Schaller, *Phys. Rev. A* **85**, 062118 (2012).
- [18] J. M. Höfener, G. C. Sethia, and T. Gross, *Phil. Trans. R. Soc. A* **371**, 1999 (2013).
- [19] D. Vitali, P. Tombesi, and G. J. Milburn, *Phys. Rev. A* **57**, 4930 (1998).
- [20] N. Ganesan and T.-J. Tarn, *Phys. Rev. A* **75**, 032323 (2007).
- [21] J. Zhang, R.-B. Wu, C.-W. Li, and T.-J. Tarn, *IEEE Trans. Automat. Contr.* **55**, 619 (2010).
- [22] G. F. Zhang and M. R. James, *IEEE Trans. Automat. Contr.* **56**, 1535 (2011).
- [23] B. Qi and L. Guo, *Sys. Contr. Lett.* **59**, 333 (2010).
- [24] R. Vijay, C. Macklin, D. H. Slichter, S. J. Weber, K. W. Murch, R. Naik, A. N. Korotkov, and I. Siddiqi, *Nature (London)* **490**, 77 (2012).
- [25] C. Ahn, A. C. Doherty, and A. J. Landahl, *Phys. Rev. A* **65**, 042301 (2002); J. Kerckhoff, H. I. Nurdin, D. S. Pavlichin, and H. Mabuchi, *Phys. Rev. Lett.* **105**, 040502 (2010).
- [26] S.-B. Xue, R.-B. Wu, W.-M. Zhang, J. Zhang, C.-W. Li, and T.-J. Tarn, *Phys. Rev. A* **86**, 052304 (2012).
- [27] J. Wang, H. M. Wiseman, and G. J. Milburn, *Phys. Rev. A* **71**, 042309 (2005).
- [28] N. Yamamoto, K. Tsumura, and S. Hara, *Automatica* **43**, 981 (2007).
- [29] Z. Liu, L. L. Kuang, K. Hu, L. T. Xu, S. H. Wei, L. Z. Guo, and X. Q. Li, *Phys. Rev. A* **82**, 032335 (2010).
- [30] A. Hopkins, K. Jacobs, S. Habib, and K. C. Schwab, *Phys. Rev. B* **68**, 235328 (2003).
- [31] J. Zhang, Y.-X. Liu, and F. Nori, *Phys. Rev. A* **79**, 052102 (2009).
- [32] Ya. S. Greenberg, E. Ilchev, and F. Nori, *Phys. Rev. B* **80**, 214423 (2009); K. Xia and J. Evers, *ibid.* **82**, 184532 (2010).
- [33] M. J. Woolley, A. C. Doherty, and G. J. Milburn, *Phys. Rev. B* **82**, 094511 (2010).
- [34] J. Combes and K. Jacobs, *Phys. Rev. Lett.* **96**, 010504 (2006); J. Combes, H. M. Wiseman, and K. Jacobs, *ibid.* **100**, 160503 (2008).
- [35] J. Zhang, Y.-X. Liu, R.-B. Wu, C.-W. Li, and T.-J. Tarn, *Phys. Rev. A* **82**, 022101 (2010).
- [36] H. M. Wiseman and G. J. Milburn, *Phys. Rev. Lett.* **70**, 548 (1993); H. M. Wiseman, *Phys. Rev. A* **49**, 2133 (1994).
- [37] H. Mabuchi and A. C. Doherty, *Science* **298**, 1372 (2002).
- [38] A. C. Doherty, S. Habib, K. Jacobs, H. Mabuchi, and S. M. Tan, *Phys. Rev. A* **62**, 012105 (2000).
- [39] S. Mancini, *Phys. Rev. A* **73**, 010304(R) (2006).
- [40] H. M. Wiseman and G. J. Milburn, *Phys. Rev. A* **49**, 4110 (1994).
- [41] S. Lloyd, *Phys. Rev. A* **62**, 022108 (2000).
- [42] M. R. James, H. I. Nurdin, and I. R. Petersen, *IEEE Trans. Automat. Contr.* **53**, 1787 (2008).
- [43] M. Yanagisawa and H. Kimura, *IEEE Trans. Automat. Contr.* **48**, 2107 (2003).
- [44] J. Gough and M. R. James, *IEEE Trans. Automat. Contr.* **54**, 2530 (2009).
- [45] D. Riste, C. C. Bultink, K. W. Lehnert, and L. DiCarlo, *Phys. Rev. Lett.* **109**, 240502 (2012).
- [46] F. Sciarrino, M. Ricci, F. De Martini, R. Filip, and L. Mišta, Jr., *Phys. Rev. Lett.* **96**, 020408 (2006).
- [47] S. Brakhane, W. Alt, T. Kampschulte, M. Martinez-Dorantes, R. Reimann, S. Yoon, A. Widera, and D. Meschede, *Phys. Rev. Lett.* **109**, 173601 (2012).

- [48] H. Yonezawa, D. Nakane, T. A. Wheatley, K. Iwasawa, S. Takeda, H. Arao, K. Ohki, K. Tsumura, D. W. Berry, T. C. Ralph, H. M. Wiseman, E. H. Huntington, and A. Furusawa, *Science* **337**, 1514 (2012).
- [49] J. Gieseler, B. Deutsch, R. Quidant, and L. Novotny, *Phys. Rev. Lett.* **109**, 103603 (2012).
- [50] D. W. Berry and H. M. Wiseman, *Phys. Rev. Lett.* **85**, 5098 (2000).
- [51] A. Kubanek, M. Koch, C. Sames, A. Ourjoumtsev, P. W. H. Pinkse, K. Murr, and G. Rempe, *Nature (London)* **462**, 898 (2009).
- [52] C. Sayrin, I. Dotsenko, X. Zhou, B. Peaudecerf, T. Rybarczyk, S. Gleyzes, P. Rouchon, M. Mirrahimi, H. Amini, M. Brune, J. M. Raimond, and S. Haroche, *Nature (London)* **477**, 73 (2011).
- [53] X. Zhou, I. Dotsenko, B. Peaudecerf, T. Rybarczyk, C. Sayrin, S. Gleyzes, J. M. Raimond, M. Brune, and S. Haroche, *Phys. Rev. Lett.* **108**, 243602 (2012).
- [54] R. J. Nelson, Y. Weinstein, D. Cory, and S. Lloyd, *Phys. Rev. Lett.* **85**, 3045 (2000).
- [55] H. Mabuchi, *Phys. Rev. A* **78**, 032323 (2008).
- [56] Z. F. Zhou, C. J. Liu, Y. M. Fang, J. Zhou, R. T. Glasser, L. Q. Chen, J. T. Jing, and W. P. Zhang, *Appl. Phys. Lett.* **101**, 191113 (2012).
- [57] J. Kerckhoff and K. W. Lehnert, *Phys. Rev. Lett.* **109**, 153602 (2012).
- [58] S. Iida, M. Yukawa, H. Yonezawa, N. Yamamoto, and A. Furusawa, *IEEE Trans. Automat. Contr.* **57**, 2045 (2012).
- [59] D. Jaksch, C. Bruder, J. I. Cirac, C. W. Gardiner, and P. Zoller, *Phys. Rev. Lett.* **81**, 3108 (1998).
- [60] K. M. Birnbaum, A. Boca, R. Miller, A. D. Boozer, T. E. Northup, and H. J. Kimble, *Nature (London)* **436**, 87 (2005).
- [61] J. M. Fink, M. Goppl, M. Baur, R. Bianchetti, A. Leek, P. J. Blais, and A. Wallraff, *Nature (London)* **454**, 315 (2008).
- [62] L. S. Bishop, J. M. Chow, J. Koch, A. A. Houck, M. H. Devoret, E. Thuneberg, S. M. Girvin, and R. J. Schoelkopf, *Nat. Phys.* **5**, 105 (2009).
- [63] A. Politi, J. C. F. Matthews, and J. L. O'Brien, *Science* **325**, 1221 (2009).
- [64] J. C. F. Matthews, A. Politi, A. Stefanov, and J. L. O'Brien, *Nat. Photonics* **3**, 346 (2009).
- [65] D. W. Berry and H. M. Wiseman, *Nat. Photonics* **3**, 317 (2009).
- [66] J. Zhang, R.-B. Wu, Y.-X. Liu, C.-W. Li, and T.-J. Tarn, *IEEE Trans. Automat. Contr.* **57**, 1997 (2012).
- [67] A. J. Hoffman, S. J. Srinivasan, S. Schmidt, L. Spietz, J. Aumentado, H. E. Türeci, and A. A. Houck, *Phys. Rev. Lett.* **107**, 053602 (2011).
- [68] P. D. Nation, M. P. Blencowe, and E. Buks, *Phys. Rev. B* **78**, 104516 (2008).
- [69] I. Tornes and D. Stroud, *Phys. Rev. B* **77**, 224513 (2008).
- [70] I. Buluta, S. Ashhab, and F. Nori, *Rep. Prog. Phys.* **74**, 104401 (2011).
- [71] I. Georgescu and F. Nori, *Phys. World* **25**, 16 (2012).
- [72] I. Buluta and F. Nori, *Science* **326**, 108 (2009).
- [73] P. D. Nation, J. R. Johansson, M. P. Blencowe, and F. Nori, *Rev. Mod. Phys.* **84**, 1 (2012).
- [74] J. Q. You and F. Nori, *Phys. Today* **58**, 42 (2005).
- [75] J. Q. You and F. Nori, *Nature (London)* **474**, 589 (2011).
- [76] Z.-L. Xiang, S. Ashhab, J. Q. You, and F. Nori, *Rev. Mod. Phys.* **85**, 623 (2013).
- [77] A detailed and pedagogical derivation of the input-output formalism can be found in K. Jacobs, [arXiv:quant-ph/9810015](https://arxiv.org/abs/quant-ph/9810015).
- [78] C. W. Gardiner and M. J. Collett, *Phys. Rev. A* **31**, 3761 (1985); C. W. Gardiner and P. Zoller, *Quantum Noise*, 3rd ed. (Springer-Verlag, Berlin, 2004).
- [79] J. E. Gough, *Phys. Rev. A* **78**, 052311 (2008).
- [80] R. I. Hudson and K. R. Parthasarathy, *Commun. Math. Phys.* **93**, 301 (1984).
- [81] G. Wendin and V. S. Shumeiko, in *Handbook of Theoretical and Computational Nanotechnology*, edited by M. Rieth and W. Schommers (ASP, Los Angeles, 2006), Vol. 3, pp. 223–309.
- [82] M. A. Castellanos-Beltran, K. D. Irwin, G. C. Hilton, L. R. Vale, and K. W. Lehnert, *Nature Phys.* **4**, 929 (2008).
- [83] Y.-X. Liu, A. Miranowicz, Y. B. Gao, J. Bajer, C. P. Sun, and F. Nori, *Phys. Rev. A* **82**, 032101 (2010).
- [84] H. M. Gibbs, S. L. McCall, and T. N. C. Venkatesan, *Phys. Rev. Lett.* **36**, 1135 (1976).
- [85] G. Rempe, R. J. Thompson, R. J. Brecha, W. D. Lee, and H. J. Kimble, *Phys. Rev. Lett.* **67**, 1727 (1991).
- [86] J. A. Sauer, K. M. Fortier, M. S. Chang, C. D. Hamley, and M. S. Chapman, *Phys. Rev. A* **69**, 051804 (2004).
- [87] S. Gupta, K. L. Moore, K. W. Murch, and D. M. Stamper-Kurn, *Phys. Rev. Lett.* **99**, 213601 (2007).
- [88] F. Brennecke, S. Ritter, T. Donner, and T. Esslinger, *Science* **322**, 235 (2008).
- [89] Y. F. Xiao, Ş. K. Özdemir, V. Gaddam, C. H. Dong, N. Imoto, and L. Yang, *Opt. Express* **16**, 21462 (2008).
- [90] H. Wang, H. C. Sun, J. Zhang, and Y.-X. Liu, *Science China* **55**, 2264 (2012).
- [91] R. R. Puri, *Mathematical Methods of Quantum Optics* (Springer-Verlag, Berlin, 2001).
- [92] A. Miranowicz, M. Paprzycka, Y.-X. Liu, J. Bajer, and F. Nori, *Phys. Rev. A* **87**, 023809 (2013).
- [93] X. W. Xu and Y. J. Li, *J. Phys. B* **46**, 035502 (2013).